PERGAMON

International Journal of Solids and Structures 40 (2003) 5689–5705

INTERNATIONAL JOURNAL OF SOLIDS and STRUCTURES

www.elsevier.com/locate/ijsolstr

Alternative state space formulations for magnetoelectric thermoelasticity with transverse isotropy and the application to bending analysis of nonhomogeneous plates

W.Q. Chen [a,*], Kang Yong Lee [b,*]

[a] *Department of Civil Engineering, Zhejiang University, Zheda Road 38, Hangzhou 310027, PR China*
[b] *School of Mechanical Engineering, Yonsei University, Seoul 120-749, South Korea*

Received 3 March 2003; received in revised form 10 June 2003

Abstract

By introducing two displacement functions and two stress functions, the governing equations of the linear theory of magneto-electro-thermo-elasticity with transverse isotropy are simplified. On selecting certain physical quantities as the basic unknowns, two new state equations are established. Each of them is order reduced when compared with the one reported recently in literature, leading to a higher numerical efficiency. The material inhomogeneity along the axis of symmetry (z-direction) can be taken into account and an approximate laminate model is employed to facilitate deriving analytical solutions. The validity of new formulations is examined by considering a laminated magneto-electro-elastic rectangular plate and good agreement is obtained with existent results. A plate with a functionally graded property is then analyzed. The effect of magnetoelectric coupling in a $BaTiO_3$–$CoFe_2O_4$ composite predicted from the micro-mechanics simulation is studied quantitatively.

Keywords: Displacement function; Stress function; New state space formulation; Nonhomogeneous plate

1. Introduction

Problems of magneto-electro-elastic materials are of intensive research interest in recent years (Avellaneda and Harshe, 1994; Huang et al., 1998; Ezzat and Othman, 2000; Li, 2000; Tan and Tong, 2002; Wang and Shen, 2003), because of the coupling effects among the electric, magnetic and elastic fields, which may enable them to be a potential material for adaptive structural control. Pan (2001) first presented an exact three-dimensional analysis of a simply supported multilayered orthotropic magneto-electro-elastic plate using a propagator matrix method. Wang et al. (2003) recently proposed an exact state space approach. The two methods in Pan (2001) and Wang et al. (2003) should be essentially the

* Corresponding authors. Tel.: +86-5718-7952284; fax: +86-571-87952165 (W.Q. Chen), Tel./fax: +82-2-2123-2813 (K.Y. Lee).
E-mail addresses: chenwq@rocketmail.com (W.Q. Chen), kyl2813@yahoo.co.kr (K.Y. Lee).

0020-7683/$ - see front matter © 2003 Elsevier Ltd. All rights reserved.
doi:10.1016/S0020-7683(03)00339-1

same, but the later one is easier to be understood and also more convenient for use. From the state space formulations established by Wang et al. (2003) for orthotropic magneto-electro-elastic materials, the ones for a material with transverse isotropy can be readily written down. It is noted here that, however, more efficient state space formulations can be established through some simple mathematical substitutions, as already illustrated in piezoelasticity (Ding et al., 2000; Chen et al., 2001; Ding and Chen, 2001).

By introducing two displacement functions and two stress functions, two independent state equations are established from the three-dimensional magneto-electro-elasticity equations for transverse isotropy with thermal effect, body forces, free charge density and electric current density. In contrast to the tenth-order state equation reported recently by Wang et al. (2003), the ones presented here are with lower orders (second-order and eighth-order, respectively) and hence the computational efficiency can be improved for practical problems. More importantly, the use of the displacement and stress functions allows one to get a deep insight into the physical essence of related problems. It is noted here that the state space formulations are also valid when the material is inhomogeneous along the axis of symmetry (perpendicular to the plane of isotropy). The new state space formulations are then applied to analyze the static behaviors of a nonhomogeneous magneto-electro-elastic plate by employing an approximate laminate model. We find that closed-form solutions can be obtained not only for the simply supported conditions, as that considered by Wang et al. (2003), but also for another kind of boundary conditions, namely the rigidly slipping conditions. Numerical results of a simply supported rectangular plate with a functionally graded property are presented. As is known to all, there is no magnetoelectric coupling existing in either $BaTiO_3$ or $CoFe_2O_4$. Both Pan (2001) and Wang et al. (2003) took the magnetoelectric coefficients as zero in the analysis of a $BaTiO_3$–$CoFe_2O_4$ laminated plate. However, as pointed our by Li (2000), the micromechanics simulation showed that the magnetoelectric coupling does exist in a $BaTiO_3$–$CoFe_2O_4$ fiber reinforced or laminated plate. The effect of this coupling on the plate bending behavior will be examined in the paper numerically.

2. Basic equations

In Cartesian coordinates (with the z-axis being normal to the plane of isotropy), the constitutive relations of a transversely isotropic magneto-electro-elastic body with the thermal effect read (Li, 2000; Wang and Shen, 2003)

$$\begin{aligned}
\sigma_x &= c_{11}\frac{\partial u}{\partial x} + c_{12}\frac{\partial v}{\partial y} + c_{13}\frac{\partial w}{\partial z} + e_{31}\frac{\partial \phi}{\partial z} + q_{31}\frac{\partial \psi}{\partial z} - \beta_1 T,\\
\sigma_y &= c_{12}\frac{\partial u}{\partial x} + c_{11}\frac{\partial v}{\partial y} + c_{13}\frac{\partial w}{\partial z} + e_{31}\frac{\partial \phi}{\partial z} + q_{31}\frac{\partial \psi}{\partial z} - \beta_1 T,\\
\sigma_z &= c_{13}\frac{\partial u}{\partial x} + c_{13}\frac{\partial v}{\partial y} + c_{33}\frac{\partial w}{\partial z} + e_{33}\frac{\partial \phi}{\partial z} + q_{33}\frac{\partial \psi}{\partial z} - \beta_3 T,\\
\tau_{xz} &= c_{44}\left(\frac{\partial u}{\partial z} + \frac{\partial w}{\partial x}\right) + e_{15}\frac{\partial \phi}{\partial x} + q_{15}\frac{\partial \psi}{\partial x},\\
\tau_{yz} &= c_{44}\left(\frac{\partial v}{\partial z} + \frac{\partial w}{\partial y}\right) + e_{15}\frac{\partial \phi}{\partial y} + q_{15}\frac{\partial \psi}{\partial y},\\
\tau_{xy} &= c_{66}\left(\frac{\partial u}{\partial y} + \frac{\partial v}{\partial x}\right),
\end{aligned} \tag{1}$$

$$
\begin{aligned}
D_x &= e_{15}\left(\frac{\partial u}{\partial z}+\frac{\partial w}{\partial x}\right)-\varepsilon_{11}\frac{\partial \phi}{\partial x}-d_{11}\frac{\partial \psi}{\partial x},\\
D_y &= e_{15}\left(\frac{\partial v}{\partial z}+\frac{\partial w}{\partial y}\right)-\varepsilon_{11}\frac{\partial \phi}{\partial y}-d_{11}\frac{\partial \psi}{\partial y},\\
D_z &= e_{31}\frac{\partial u}{\partial x}+e_{31}\frac{\partial v}{\partial y}+e_{33}\frac{\partial w}{\partial z}-\varepsilon_{33}\frac{\partial \phi}{\partial z}-d_{33}\frac{\partial \psi}{\partial z}+p_3T,
\end{aligned}
\tag{2}
$$

$$
\begin{aligned}
B_x &= q_{15}\left(\frac{\partial u}{\partial z}+\frac{\partial w}{\partial x}\right)-d_{11}\frac{\partial \phi}{\partial x}-\mu_{11}\frac{\partial \psi}{\partial x},\\
B_y &= q_{15}\left(\frac{\partial v}{\partial z}+\frac{\partial w}{\partial y}\right)-d_{11}\frac{\partial \phi}{\partial y}-\mu_{11}\frac{\partial \psi}{\partial y},\\
B_z &= q_{31}\frac{\partial u}{\partial x}+q_{31}\frac{\partial v}{\partial y}+q_{33}\frac{\partial w}{\partial z}-d_{33}\frac{\partial \phi}{\partial z}-\mu_{33}\frac{\partial \psi}{\partial z}+m_3T,
\end{aligned}
\tag{3}
$$

where, ϕ, ψ, D_i, B_i and T are the electric potential, magnetic potential, electric displacement components, magnetic induction components, and the incremental temperature, respectively; σ_i and τ_{ij} are the normal and shear stresses, respectively; u, v and w are components of the mechanical displacement in x-, y- and z-directions, respectively; c_{ij}, ε_{ij}, e_{ij}, q_{ij}, d_{ij}, μ_{ij}, p_3 and m_3 are the elastic, dielectric, piezoelectric, piezomagnetic, magnetoelectric, magnetic, pyroelectric and pyromagnetic constants, respectively; β_i are the thermal modules. Note that we have an additional relation $c_{11}=c_{12}+2c_{66}$ for transverse isotropy. In this paper, all these material constants are assumed to be functions of the coordinate z. The governing equations are

$$
\begin{aligned}
&\frac{\partial \sigma_x}{\partial x}+\frac{\partial \tau_{xy}}{\partial y}+\frac{\partial \tau_{xz}}{\partial z}+F_x=0,\\
&\frac{\partial \tau_{xy}}{\partial x}+\frac{\partial \sigma_y}{\partial y}+\frac{\partial \tau_{yz}}{\partial z}+F_y=0,\\
&\frac{\partial \tau_{xz}}{\partial x}+\frac{\partial \tau_{yz}}{\partial y}+\frac{\partial \sigma_z}{\partial z}+F_z=0,
\end{aligned}
\tag{4}
$$

$$
\frac{\partial D_x}{\partial x}+\frac{\partial D_y}{\partial y}+\frac{\partial D_z}{\partial z}=f_{\mathrm{e}},
\tag{5}
$$

$$
\frac{\partial B_x}{\partial x}+\frac{\partial B_y}{\partial y}+\frac{\partial B_z}{\partial z}=f_{\mathrm{m}},
\tag{6}
$$

where F_i are components of the body force, f_{e} is the free charge density, and f_{m} the electric current density (or magnetic charge density). The temperature distribution usually can be determined a priori from the corresponding temperature field equation, thus it is assumed known throughout this paper.

Following a routine method (Fan and Ye, 1990; Lee and Jiang, 1996; Chen et al., 1998; Tarn, 2002; Wang et al., 2003), the conventional state equation involving effects of body force, free charge density, electric current density and temperature change as well as the material inhomogeneity along z-direction is obtained from Eqs. (1)–(6) as follows

$$\frac{\partial}{\partial z}\begin{Bmatrix} u \\ v \\ D_z \\ B_z \\ \sigma_z \\ \tau_{xz} \\ \tau_{yz} \\ \phi \\ \psi \\ w \end{Bmatrix} = \begin{bmatrix} \mathbf{0} & \mathbf{A}_1 \\ \mathbf{A}_2 & \mathbf{0} \end{bmatrix} \begin{Bmatrix} u \\ v \\ D_z \\ B_z \\ \sigma_z \\ \tau_{xz} \\ \tau_{yz} \\ \phi \\ \psi \\ w \end{Bmatrix} + \begin{Bmatrix} 0 \\ 0 \\ f_e \\ f_m \\ -F_z \\ -F_x - k_5 \dfrac{\partial T}{\partial x} \\ -F_y - k_5 \dfrac{\partial T}{\partial y} \\ l_2 T \\ l_3 T \\ l_1 T \end{Bmatrix}, \tag{7}$$

where the matrices $\mathbf{A}_1$ and $\mathbf{A}_2$ can be deduced from Eqs. (11) and (12) in Wang et al. (2003) by simply setting $c_{11} = c_{22}$, $c_{13} = c_{23}$, $c_{44} = c_{55}$, $e_{31} = e_{32}$, $e_{24} = e_{15}$, $\varepsilon_{11} = \varepsilon_{22}$, $q_{31} = q_{32}$, $q_{24} = q_{15}$, $d_{11} = d_{22}$, and $\mu_{11} = \mu_{22}$. In our notation, they are

$$\mathbf{A}_1 = \begin{bmatrix} \dfrac{1}{c_{44}} & 0 & -\dfrac{e_{15}}{c_{44}}\dfrac{\partial}{\partial x} & -\dfrac{q_{15}}{c_{44}}\dfrac{\partial}{\partial x} & -\dfrac{\partial}{\partial x} \\ & \dfrac{1}{c_{44}} & -\dfrac{e_{15}}{c_{44}}\dfrac{\partial}{\partial y} & -\dfrac{q_{15}}{c_{44}}\dfrac{\partial}{\partial y} & -\dfrac{\partial}{\partial y} \\ & & k_1\Lambda & k_2\Lambda & 0 \\ & \text{sym.} & & k_3\Lambda & 0 \\ & & & & 0 \end{bmatrix},$$

$$\mathbf{A}_2 = \begin{bmatrix} k_4\dfrac{\partial^2}{\partial x^2} - c_{66}\dfrac{\partial^2}{\partial y^2} & (k_4 + c_{66})\dfrac{\partial^2}{\partial x \partial y} & -g_2\dfrac{\partial}{\partial x} & -g_3\dfrac{\partial}{\partial x} & -g_1\dfrac{\partial}{\partial x} \\ & k_4\dfrac{\partial^2}{\partial y^2} - c_{66}\dfrac{\partial^2}{\partial x^2} & -g_2\dfrac{\partial}{\partial y} & -g_3\dfrac{\partial}{\partial y} & -g_1\dfrac{\partial}{\partial y} \\ & & \dfrac{\alpha_{22}}{\alpha} & \dfrac{\alpha_{23}}{\alpha} & \dfrac{\alpha_{12}}{\alpha} \\ & \text{sym.} & & \dfrac{\alpha_{33}}{\alpha} & \dfrac{\alpha_{13}}{\alpha} \\ & & & & \dfrac{\alpha_{11}}{\alpha} \end{bmatrix}, \tag{8}$$

where $\Lambda = \partial^2/\partial x^2 + \partial^2/\partial y^2$, "sym." indicates a symmetric matrix, and the following definitions have been employed in Eqs. (7) and (8)

$$k_1 = \varepsilon_{11} + e_{15}^2/c_{44}, \quad k_2 = d_{11} + e_{15}q_{15}/c_{44}, \quad k_3 = \mu_{11} + q_{15}^2/c_{44}, \quad k_4 = c_{13}g_1 + e_{31}g_2 + q_{31}g_3 - c_{11},$$
$$k_5 = c_{13}l_1 + e_{31}l_2 + q_{31}l_3 - \beta_1,$$

$$g_i = (c_{13}\alpha_{1i} + e_{31}\alpha_{2i} + q_{31}\alpha_{3i})/\alpha, \quad l_i = (\beta_3\alpha_{1i} - p_3\alpha_{2i} - m_3\alpha_{3i})/\alpha, \tag{9}$$

$$\alpha = \begin{vmatrix} c_{33} & e_{33} & q_{33} \\ e_{33} & -\varepsilon_{33} & -d_{33} \\ q_{33} & -d_{33} & -\mu_{33} \end{vmatrix}$$

and α_{ij} are the corresponding algebraic cofactors of α with $\alpha_{ij} = \alpha_{ji}$.

3. New formulations for state space approach

To construct new state space formulations, the following substitutions are employed (Ding et al., 2000)

$$\begin{aligned} u &= -\frac{\partial \Psi}{\partial y} - \frac{\partial G}{\partial x}, \quad v = \frac{\partial \Psi}{\partial x} - \frac{\partial G}{\partial y}, \\ \tau_{xz} &= -\frac{\partial \tau_1}{\partial y} - \frac{\partial \tau_2}{\partial x}, \quad \tau_{yz} = \frac{\partial \tau_1}{\partial x} - \frac{\partial \tau_2}{\partial y}, \\ F_x &= -\frac{\partial F_1}{\partial y} - \frac{\partial F_2}{\partial x}, \quad F_y = \frac{\partial F_1}{\partial x} - \frac{\partial F_2}{\partial y}, \end{aligned} \tag{10}$$

where Ψ and G are two displacement functions, τ_1 and τ_2 are two stress functions, and F_1 and F_2 are two body force functions. Note that Wang and Shen (2002) employed the decomposition formula for displacements in Eq. (10) only to derive a general solution for a transversely isotropic magneto-electro-elastic medium. Substitution of Eq. (10) into the expressions for τ_{xz} and τ_{yz} in Eq. (1), gives

$$\begin{aligned} &-\frac{\partial}{\partial y}\left[\tau_1 - c_{44}\frac{\partial \Psi}{\partial z}\right] - \frac{\partial}{\partial x}\left[\tau_2 + c_{44}w + e_{15}\phi + q_{15}\psi - c_{44}\frac{\partial G}{\partial z}\right] = 0, \\ &\frac{\partial}{\partial x}\left[\tau_1 - c_{44}\frac{\partial \Psi}{\partial z}\right] - \frac{\partial}{\partial y}\left[\tau_2 + c_{44}w + e_{15}\phi + q_{15}\psi - c_{44}\frac{\partial G}{\partial z}\right] = 0, \end{aligned} \tag{11}$$

which will be satisfied provided that

$$\tau_1 - c_{44}\frac{\partial \Psi}{\partial z} = 0, \tag{12}$$

$$\tau_2 + c_{44}w + e_{15}\phi + q_{15}\psi - c_{44}\frac{\partial G}{\partial z} = 0. \tag{13}$$

Substitution of Eqs. (1) and (10) into the first two equations in Eq. (4), yields

$$-\frac{\partial}{\partial y}A - \frac{\partial}{\partial x}B = 0, \quad \frac{\partial}{\partial x}A - \frac{\partial}{\partial y}B = 0, \tag{14}$$

where

$$A = c_{66}\Lambda\Psi + \frac{\partial \tau_1}{\partial z} + F_1, \tag{15}$$

$$B = c_{11}\Lambda G - c_{13}\frac{\partial w}{\partial z} - e_{31}\frac{\partial \phi}{\partial z} - q_{31}\frac{\partial \psi}{\partial z} + \frac{\partial \tau_2}{\partial z} + \beta_1 T + F_2. \tag{16}$$

Similar to the demonstration outlined in Appendix A in Ding et al. (1996), one can obtain from Eq. (14)

$$A = 0, \tag{17}$$

$$B = 0. \tag{18}$$

Utilizing Eq. (10), one obtains from the third equations of Eqs. (1)–(4), as well as Eqs. (5) and (6)

$$c_{33}\frac{\partial w}{\partial z} + e_{33}\frac{\partial \phi}{\partial z} + q_{33}\frac{\partial \psi}{\partial z} = \sigma_z + c_{13}\Lambda G + \beta_3 T, \tag{19}$$

$$e_{33}\frac{\partial w}{\partial z} - \varepsilon_{33}\frac{\partial \phi}{\partial z} - d_{33}\frac{\partial \psi}{\partial z} = D_z + e_{31}\Lambda G - p_3 T, \tag{20}$$

$$q_{33}\frac{\partial w}{\partial z}-d_{33}\frac{\partial \phi}{\partial z}-\mu_{33}\frac{\partial \psi}{\partial z}=B_z+q_{31}\Lambda G-m_3T, \tag{21}$$

$$\frac{\partial \sigma_z}{\partial z}=\Lambda\tau_2-F_z, \tag{22}$$

$$\frac{\partial D_z}{\partial z}=e_{15}\Lambda\frac{\partial G}{\partial z}-e_{15}\Lambda w+\varepsilon_{11}\Lambda\phi+d_{11}\Lambda\psi+f_{\mathrm{e}}, \tag{23}$$

$$\frac{\partial B_z}{\partial z}=q_{15}\Lambda\frac{\partial G}{\partial z}-q_{15}\Lambda w+d_{11}\Lambda\phi+\mu_{11}\Lambda\psi+f_{\mathrm{m}}. \tag{24}$$

Eqs. (12), (13) and (17)–(24) can be rearranged, after a straightforward mathematical manipulation, and written in matrix form as follows:

$$\frac{\partial}{\partial z}\begin{Bmatrix}\Psi\\ \tau_1\end{Bmatrix}=\begin{bmatrix}0 & 1/c_{44}\\ -c_{66}\Lambda & 0\end{bmatrix}\begin{Bmatrix}\Psi\\ \tau_1\end{Bmatrix}+\begin{Bmatrix}0\\ -F_1\end{Bmatrix}, \tag{25}$$

$$\frac{\partial}{\partial z}\begin{Bmatrix}G\\ \sigma_z\\ D_z\\ B_z\end{Bmatrix}=\begin{bmatrix}\dfrac{1}{c_{44}} & 1 & \dfrac{e_{15}}{c_{44}} & \dfrac{q_{15}}{c_{44}}\\ \Lambda & 0 & 0 & 0\\ \dfrac{e_{15}}{c_{44}}\Lambda & 0 & k_1\Lambda & k_2\Lambda\\ \dfrac{q_{15}}{c_{44}}\Lambda & 0 & k_2\Lambda & k_3\Lambda\end{bmatrix}\begin{Bmatrix}\tau_2\\ w\\ \phi\\ \psi\end{Bmatrix}+\begin{Bmatrix}0\\ -F_z\\ f_{\mathrm{e}}\\ f_{\mathrm{m}}\end{Bmatrix}, \tag{26}$$

$$\frac{\partial}{\partial z}\begin{Bmatrix}\tau_2\\ w\\ \phi\\ \psi\end{Bmatrix}=\begin{bmatrix}k_4\Lambda & g_1 & g_2 & g_3\\ g_1\Lambda & \dfrac{\alpha_{11}}{\alpha} & \dfrac{\alpha_{12}}{\alpha} & \dfrac{\alpha_{13}}{\alpha}\\ g_2\Lambda & \dfrac{\alpha_{12}}{\alpha} & \dfrac{\alpha_{22}}{\alpha} & \dfrac{\alpha_{23}}{\alpha}\\ g_3\Lambda & \dfrac{\alpha_{13}}{\alpha} & \dfrac{\alpha_{23}}{\alpha} & \dfrac{\alpha_{33}}{\alpha}\end{bmatrix}\begin{Bmatrix}G\\ \sigma_z\\ D_z\\ B_z\end{Bmatrix}+\begin{Bmatrix}k_5T-F_2\\ l_1T\\ l_2T\\ l_3T\end{Bmatrix}, \tag{27}$$

where the notations defined in Eq. (9) have been employed. We still have the following equations to determine the other variables

$$\begin{aligned}
&\sigma_x+\sigma_y=2(k_4+c_{66})\Lambda G+2g_1\sigma_z+2g_2D_z+2g_3B_z+2k_5T,\\
&\sigma_x-\sigma_y=-2c_{66}\left[2\frac{\partial^2\Psi}{\partial x\,\partial y}+\left(\frac{\partial^2}{\partial x^2}-\frac{\partial^2}{\partial y^2}\right)G\right],\\
&\tau_{xy}=c_{66}\left[\left(\frac{\partial^2}{\partial x^2}-\frac{\partial^2}{\partial y^2}\right)\Psi-2\frac{\partial^2 G}{\partial x\,\partial y}\right],\\
&D_x=-\frac{e_{15}}{c_{44}}\frac{\partial\tau_1}{\partial y}-\frac{\partial}{\partial x}\left(k_1\phi+k_2\psi+\frac{e_{15}}{c_{44}}\tau_2\right),\\
&D_y=\frac{e_{15}}{c_{44}}\frac{\partial\tau_1}{\partial x}-\frac{\partial}{\partial y}\left(k_1\phi+k_2\psi+\frac{e_{15}}{c_{44}}\tau_2\right),\\
&B_x=-\frac{q_{15}}{c_{44}}\frac{\partial\tau_1}{\partial y}-\frac{\partial}{\partial x}\left(k_2\phi+k_3\psi+\frac{q_{15}}{c_{44}}\tau_2\right),\\
&B_y=\frac{q_{15}}{c_{44}}\frac{\partial\tau_1}{\partial x}-\frac{\partial}{\partial y}\left(k_2\phi+k_3\psi+\frac{q_{15}}{c_{44}}\tau_2\right).
\end{aligned} \tag{28}$$

As shown in Eqs. (25)–(27), the 10 basic variables (or state variables) Ψ, τ_1, G, σ_z, D_z, B_z, τ_2, w, ϕ and ψ are dropped into three groups: one is only related to Ψ and τ_1 and the other two ones coupled by the remnant eight state variables. It is obvious that either Eq. (25) or the one coupled by Eqs. (26) and (27) has an order lower than Eq. (7), leading to a somehow higher numerical efficiency. Furthermore, the separation of state equations will clearly show some particular characteristics occupied by practical problems that cannot be revealed by the tenth-order state equation. For example, the first group characterized by Ψ and τ_1 is independent of the electric and magnetic potentials and relates to the elastic in-plane deformation only. Also, for the bending of a plate, it is only necessary to solve Eqs. (26) and (27), the total order of which is eight, instead of the tenth one, Eq. (7).

Another superiority of the new formulations is that relative simpler operators are involved. As can be seen, the right-hand sides of Eqs. (25)–(27) include the operator Λ only, which enables us to write down directly the corresponding formulations in circular cylindrical coordinates (r, θ, z). In fact, Eqs. (25)–(27) are still valid except for

$$\Lambda = \partial^2/\partial r^2 + r\partial/\partial r + \partial^2/(r^2\partial\theta^2),$$

while the separation formulae in Eq. (10) should be replaced by

$$\begin{aligned}
&u_r = -\frac{1}{r}\frac{\partial\Psi}{\partial\theta} - \frac{\partial G}{\partial r}, \quad u_\theta = \frac{\partial\Psi}{\partial r} - \frac{1}{r}\frac{\partial G}{\partial\theta},\\
&\tau_{rz} = -\frac{1}{r}\frac{\partial\tau_1}{\partial\theta} - \frac{\partial\tau_2}{\partial r}, \quad \tau_{\theta z} = \frac{\partial\tau_1}{\partial r} - \frac{1}{r}\frac{\partial\tau_2}{\partial\theta},\\
&F_r = -\frac{1}{r}\frac{\partial F_1}{\partial\theta} - \frac{\partial F_2}{\partial r}, \quad F_\theta = \frac{\partial F_1}{\partial r} - \frac{1}{r}\frac{\partial F_2}{\partial\theta}.
\end{aligned} \tag{29}$$

Correspondingly, Eq. (28) becomes

$$\begin{aligned}
&\sigma_r + \sigma_\theta = 2(k_4 + c_{66})\Lambda G + 2g_1\sigma_z + 2g_2 D_z + 2g_3 B_z + 2k_5 T,\\
&\sigma_r - \sigma_\theta = -2c_{66}\left[2\frac{\partial}{\partial r}\left(\frac{1}{r}\frac{\partial\Psi}{\partial\theta}\right) + \frac{\partial^2 G}{\partial r^2} - \frac{1}{r}\frac{\partial G}{\partial r} - \frac{1}{r^2}\frac{\partial^2 G}{\partial\theta^2}\right],\\
&\tau_{r\theta} = c_{66}\left[\frac{\partial^2\Psi}{\partial r^2} - \frac{\partial\Psi}{r\partial r} - \frac{\partial^2\Psi}{r^2\partial\theta^2} - 2\frac{\partial}{\partial r}\left(\frac{\partial G}{r\partial\theta}\right)\right],\\
&D_r = -\frac{e_{15}}{c_{44}}\frac{1}{r}\frac{\partial\tau_1}{\partial\theta} - \frac{\partial}{\partial r}\left(k_1\phi + k_2\psi + \frac{e_{15}}{c_{44}}\tau_2\right),\\
&D_\theta = \frac{e_{15}}{c_{44}}\frac{\partial\tau_1}{\partial r} - \frac{1}{r}\frac{\partial}{\partial\theta}\left(k_1\phi + k_2\psi + \frac{e_{15}}{c_{44}}\tau_2\right),\\
&B_r = -\frac{q_{15}}{c_{44}}\frac{1}{r}\frac{\partial\tau_1}{\partial\theta} - \frac{\partial}{\partial r}\left(k_2\phi + k_3\psi + \frac{q_{15}}{c_{44}}\tau_2\right),\\
&B_\theta = \frac{q_{15}}{c_{44}}\frac{\partial\tau_1}{\partial r} - \frac{1}{r}\frac{\partial}{\partial\theta}\left(k_2\phi + k_3\psi + \frac{q_{15}}{c_{44}}\tau_2\right).
\end{aligned} \tag{30}$$

In the next section, the bending of a nonhomogeneous transversely isotropic rectangular magneto-electro-elastic plate that has arbitrarily distributed material properties along the thickness direction will be considered.

4. Analysis of nonhomogeneous rectangular plates

Consider a transversely isotropic rectangular plate of width a, length b and thickness H, Fig. 1a. The plate is inhomogeneous along z-direction, with the isotropic plane parallel to the middle plane. We first assume that the plate is simply supported at all four straight edges, and in the end of this section, several other possible boundary conditions, for which three-dimensional solutions can be derived, will also be discussed.

If we neglect the thermal effect, the body forces, the free charge density, as well as the electric current density, the inhomogeneous terms in Eqs. (25)–(27) vanish. It is assumed that

$$\begin{bmatrix} \Psi \\ \tau_1 \end{bmatrix} = \sum_{m=0}^{\infty}\sum_{n=0}^{\infty} \begin{Bmatrix} H^2\overline{\Psi}(\zeta) \\ Hc_{44}^0\overline{\tau}_1(\zeta) \end{Bmatrix} \cos(m\pi\xi)\cos(n\pi\eta), \tag{31}$$

$$\begin{Bmatrix} G \\ \sigma_z \\ D_z \\ B_z \\ \tau_2 \\ w \\ \phi \\ \psi \end{Bmatrix} = \sum_{m=1}^{\infty}\sum_{n=1}^{\infty} \begin{Bmatrix} H^2\overline{G}(\zeta)/J_{mn} \\ c_{44}^0\overline{\sigma}_z(\zeta) \\ \sqrt{c_{44}^0\varepsilon_{33}^0}\overline{D}_z(\zeta) \\ \sqrt{c_{44}^0\mu_{33}^0}\overline{B}_z(\zeta) \\ Hc_{44}^0\overline{\tau}_2(\zeta) \\ H\overline{w}(\zeta) \\ H\sqrt{c_{44}^0/\varepsilon_{33}^0}\overline{\phi}(\zeta) \\ H\sqrt{c_{44}^0/\mu_{33}^0}\overline{\psi}(\zeta) \end{Bmatrix} \sin(m\pi\xi)\sin(n\pi\eta), \tag{32}$$

where $\zeta = z/H$, $\xi = x/a$ and $\eta = y/b$ are the dimensionless coordinates, $J_{mn} = -(s_1^2 + s_2^2)$, $s_1 = (H/a)m\pi$, $s_2 = (H/b)n\pi$, and c_{44}^0, e_{33}^0 and ε_{33}^0, etc. represent the material constants at $z = 0$. According to Eqs. (31) and (32), the following boundary conditions are satisfied at the edges

$$x = 0, \quad a : w = \sigma_x = v = \phi = \psi = 0 \quad \text{and} \quad y = 0, \quad b : w = \sigma_y = u = \phi = \psi = 0. \tag{33}$$

This type of boundary conditions is a generalization of the simply supported ones for elastic plates in a three-dimensional form (Pagano, 1970). It further requires that both the electric and magnetic potentials should be zero at the edges for the current problem. It should be noted that the simply supported conditions defined by Eq. (16) in Wang et al. (2003) are not correct in a strict sense. For example, D_z, B_z, σ_z and τ_{zy} should not appear in the boundary expressions at $x = 0$.

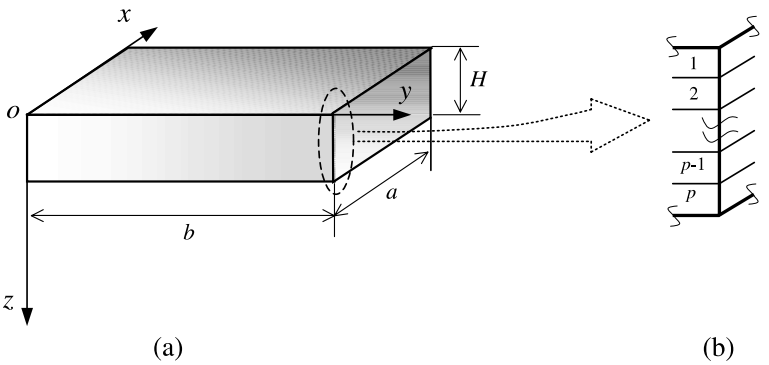

Fig. 1. A nonhomogeneous rectangular plate and the laminate model.

Substituting Eqs. (31) and (32) into Eqs. (25)–(27), making use of the orthogonal property of the trigonometric functions, one obtains for an arbitrary couple of (m,n)

$$\frac{\mathrm{d}}{\mathrm{d}\zeta}\mathbf{V}_1(\zeta)=\mathbf{M}_1\mathbf{V}_1(\zeta),\quad \frac{\mathrm{d}}{\mathrm{d}\zeta}\mathbf{V}_2(\zeta)=\mathbf{M}_2\mathbf{V}_2(\zeta), \tag{34}$$

where $\mathbf{V}_1=[\overline{\Psi},\overline{\tau}_1]^{\mathrm{T}}$, $\mathbf{V}_2=[\overline{G},\overline{\sigma}_z,\overline{D}_z,\overline{B}_z,\overline{\tau}_2,\overline{w},\overline{\phi},\overline{\psi}]^{\mathrm{T}}$, and

$$\mathbf{M}_1=\begin{bmatrix} 0 & \dfrac{c_{44}^0}{c_{44}} \\ -\dfrac{c_{66}J_{mn}}{c_{44}^0} & 0 \end{bmatrix},$$

$$\mathbf{M}_2=\begin{bmatrix}
0 & 0 & 0 & 0 & \dfrac{c_{44}^0}{c_{44}}J_{mn} & J_{mn} & \dfrac{e_{15}J_{mn}}{c_{44}}\sqrt{\dfrac{c_{44}^0}{\varepsilon_{33}^0}} & \dfrac{q_{15}J_{mn}}{c_{44}}\sqrt{\dfrac{c_{44}^0}{\mu_{33}^0}} \\
0 & 0 & 0 & 0 & & 0 & 0 & 0 \\
0 & 0 & 0 & 0 & & & \dfrac{k_1}{\varepsilon_{33}^0}J_{mn} & \dfrac{k_2J_{mn}}{\sqrt{\mu_{33}^0\varepsilon_{33}^0}} \\
0 & 0 & 0 & 0 & \text{sym.} & & & \dfrac{k_3}{\mu_{33}^0}J_{mn} \\
\dfrac{k_4}{c_{44}^0} & g_1 & g_2\sqrt{\dfrac{\varepsilon_{33}^0}{c_{44}^0}} & g_3\sqrt{\dfrac{\mu_{33}^0}{c_{44}^0}} & 0 & 0 & 0 & 0 \\
 & \dfrac{\alpha_{11}c_{44}^0}{\alpha} & \dfrac{\alpha_{12}\sqrt{c_{44}^0\varepsilon_{33}^0}}{\alpha} & \dfrac{\alpha_{13}\sqrt{c_{44}^0\mu_{33}^0}}{\alpha} & 0 & 0 & 0 & 0 \\
 & & \dfrac{\alpha_{22}\varepsilon_{33}^0}{\alpha} & \dfrac{\alpha_{23}\sqrt{\varepsilon_{33}^0\mu_{33}^0}}{\alpha} & 0 & 0 & 0 & 0 \\
\text{sym.} & & & \dfrac{\alpha_{33}\mu_{33}^0}{\alpha} & 0 & 0 & 0 & 0
\end{bmatrix}. \tag{35}$$

At this stage, two dimensionless state equations in the first-order ordinary differential form have been obtained in Eq. (34), with however, nonconstant coefficient matrices $\mathbf{M}_1$ and $\mathbf{M}_2$. It is usually difficult to find out the exact solutions of such state equations except for some particular cases of material variations along z-direction. For a general case that the material constants are arbitrary functions of z (may be different for different material constants), an efficient analysis based on the approximate laminate model, as shown in Fig. 1b, can be adopted (Tanigawa, 1995; Ding and Chen, 2001). In this method, the plate is divided into several equal thin layers, say p layers (Fig. 1b), each with a very small thickness. Thus in every layer, the material constants can be assumed constant. It is known that with the number of layers increases, the laminate model gradually approaches the actual plate and the solution will be more and more close to the exact one. In doing so, the coefficient matrices $\mathbf{M}_1$ and $\mathbf{M}_2$ become constant in the jth layer and will be denoted as $\mathbf{M}_1^j$ and $\mathbf{M}_2^j$, which have the values of $\mathbf{M}_1$ and $\mathbf{M}_2$ respectively, at $z=(j-1/2)H/p$, i.e. at the middle plane of the jth layer.

The solutions to the two state equations in Eq. (34) corresponding to the laminate model can be obtained using the matrix theory

$$\mathbf{V}_1(\zeta)=\exp[\mathbf{M}_1^j(\zeta-\zeta_j)]\mathbf{V}_1(\zeta_j),\quad (\zeta_j\leqslant\zeta\leqslant\zeta_{j+1},\ j=1,2,\ldots,p), \tag{36}$$

$$\mathbf{V}_2(\zeta)=\exp[\mathbf{M}_2^j(\zeta-\zeta_j)]\mathbf{V}_2(\zeta_j),\quad (\zeta_j\leqslant\zeta\leqslant\zeta_{j+1},\ j=1,2,\ldots,p), \tag{37}$$

where $\zeta_j = (j-1)/p$. The exponential matrix $\exp[\mathbf{M}_k^j(\zeta-\zeta_j)]$ is known as the transfer matrix that can be expressed in terms of a polynomial about the matrix $\mathbf{M}_k^j$ by virtue of the Cayley–Hamilton theorem (Bellman, 1970).

Since the basic variables should be continuous at $\zeta = \zeta_j$ $(j = 2, 3, \ldots, p)$, we obtain from Eqs. (36) and (37)

$$\mathbf{V}_1(1) = \mathbf{T}_1\mathbf{V}_1(0), \quad \mathbf{V}_2(1) = \mathbf{T}_2\mathbf{V}_2(0), \tag{38}$$

where $\mathbf{T}_1 = \prod_{j=p}^{1} \exp(\mathbf{M}_1^j/p)$ and $\mathbf{T}_2 = \prod_{j=p}^{1} \exp(\mathbf{M}_2^j/p)$ are matrices of the second-order and eighth-order, respectively.

If the plate is subjected to a combination of normal mechanical forces, electric displacements, and magnetic inductions at the top and bottom surfaces, these loads should be expanded into double Fourier series, and hence Eq. (38) can be solved in a routine way (Ding and Chen, 2001; Wang et al., 2003).

Note that after the state variables at the top surface have been obtained from Eq. (38), their values at any interior point can be calculated by

$$\mathbf{V}_k(\zeta) = \exp[\mathbf{M}_k^j(\zeta-\zeta_j)] \prod_{i=j-1}^{1} \exp[\mathbf{M}_k^i/p]\mathbf{V}_k(0), \quad (k = 1, 2;\ \zeta_j \leqslant \zeta \leqslant \zeta_{j+1}) \tag{39}$$

The induced variables are then determined from Eq. (28).

In the above, we propose an approximate three-dimensional analysis for a magneto-electro-elastic plate with material inhomogeneity along the thickness direction. For a homogeneous or laminated plate, the solution becomes completely exact as that shown in Wang et al. (2003).

Let us take a deep look at the possible boundary conditions that the above analysis can be applied similarly. If we replace the factor $\cos(m\pi\xi)\cos(n\pi\eta)$ with $\sin(m\pi\xi)\sin(n\pi\eta)$ in Eq. (31) and the factor $\sin(m\pi\xi)\sin(n\pi\eta)$ with $\cos(m\pi\xi)\cos(n\pi\eta)$ in Eq. (32), the boundary conditions at the four edges become

$$x = 0, \quad a: \tau_{xz} = \tau_{xy} = u = D_x = B_x = 0 \quad \text{and} \quad y = 0, \quad b: \tau_{yz} = \tau_{xy} = v = D_y = B_y = 0 \tag{40}$$

which correspond to the so-called rigidly slipping conditions for elastic plates. The succeeding analysis is the same as that for the simply supported conditions. Of course, the loads should also be expanded in a proper form.

It is noted here that for a plate having simple support at some edges and having rigidly slipping support at the other edges, three-dimensional solutions are also derivable. For example, when the edge $x = a$ is simply supported, and the other three edges have rigidly slipping conditions, we can assume

$$\begin{Bmatrix} \Psi \\ \tau_1 \end{Bmatrix} = \sum_{m=0}^{\infty}\sum_{n=1}^{\infty} \begin{Bmatrix} H^2\overline{\Psi}(\zeta) \\ Hc_{44}^0\overline{\tau}_1(\zeta) \end{Bmatrix} \sin\left(\frac{2m+1}{2}\pi\xi\right)\sin(n\pi\eta), \tag{41}$$

$$\begin{Bmatrix} G \\ \sigma_z \\ D_z \\ B_z \\ \tau_2 \\ w \\ \phi \\ \psi \end{Bmatrix} = \sum_{m=0}^{\infty}\sum_{n=0}^{\infty} \begin{Bmatrix} H^2\overline{G}(\zeta)/J_{mn} \\ c_{44}^0\overline{\sigma}_z(\zeta) \\ \sqrt{c_{44}^0\varepsilon_{33}^0}\,\overline{D}_z(\zeta) \\ \sqrt{c_{44}^0\mu_{33}^0}\,\overline{B}_z(\zeta) \\ Hc_{44}^0\overline{\tau}_2(\zeta) \\ H\overline{w}(\zeta) \\ H\sqrt{c_{44}^0/\varepsilon_{33}^0}\,\overline{\phi}(\zeta) \\ H\sqrt{c_{44}^0/\mu_{33}^0}\,\overline{\psi}(\zeta) \end{Bmatrix} \cos\left(\frac{2m+1}{2}\pi\xi\right)\cos(n\pi\eta). \tag{42}$$

5. Numerical results

The examples considered by Wang et al. (2003) are first checked and good agreement is obtained. The correctness of the new formulations is thus clarified. The various conclusions drawn there are not repeated here for brevity.

We then consider a simply supported nonhomogeneous magneto-electro-elastic rectangular plate with the length-to-thickness ratio $a/H = 10$ and the width-to-thickness ratio $b/H = 5$. Three types of sinusoidal loading ($m = n = 1$) applied on the top surface of the plate ($z = 0$) only are considered:

$$\text{Load 1}: \ \overline{\sigma}_z(0) = 1, \quad \text{Load 2}: \ \overline{D}_z(0) = 1, \quad \text{and Load 3}: \ \overline{B}_z(0) = 1.$$

In addition, the following functionally graded model (Reddy et al., 1999) concerning the material inhomogeneity is employed:

$$M = M^B \left(\frac{H - z}{H}\right)^{\kappa} + M^C \left[1 - \left(\frac{H - z}{H}\right)^{\kappa}\right], \tag{43}$$

where κ is the inhomogeneity parameter or gradient index, M represents an arbitrary material constant, and M^B and M^C are the material constants of $BaTiO_3$ and $CoFe_2O_4$, respectively. At the first stage, we take the material constants as exactly the same as those in Tables 1 and 2 of Wang et al. (2003), where the magnetoelectric coupling was not considered, i.e. $d_{11} = d_{33} = 0$. As regards the inhomogeneity of material, this example just considers a typical one from the theoretical view of point, although it seems that no report on functionally graded magneto-electro-electric materials can be found yet. It is believed here, however, such materials will be produced immediately, just as its counterpart of piezoelectric materials (Wu et al., 1996).

First of all, we should verify the convergence characteristics of the present method. Table 1 compares the calculated dimensionless physical quantities at the middle plane of the plate ($\zeta = 0.5$) for a 30-layer model and a 32-layer model, respectively. The inhomogeneity parameter is taken to be $\kappa = 3$. It is seen that the difference between results of the two models is completely negligible. Thus in the following, we shall take $p = 30$ and the results are believed to be highly accurate.

The variations of the nondimensional physical quantities along the thickness direction are calculated for four values of κ. The results shown in Figs. 2–4 are for Loads 1, 2 and 3, respectively. It can be seen that the material inhomogeneity has an obvious effect on the distribution of the magneto-electro-elastic field, except for σ_z when the plate is subjected to Load 1. For a laminated plate, Wang et al. (2003) also reported that there is almost no difference of σ_z for two different stacking schemes considered by them, as shown in Fig. 1d of their paper. It is noted that when $\kappa = 0$, the plate is a homogeneous $BaTiO_3$ plate and when κ tends to infinity, it becomes a homogeneous $CoFe_2O_4$ plate. Because the homogeneous $BaTiO_3$ plate has $q_{ij} = d_{ij} = 0$, the magnetic field vanishes, as shown in Figs. 2e,f and 3e,f, when it is subjected to Load 1 and

Table 1
Dimensionless physical quantities ($\zeta = 0.5$) of the plate for two laminate models

Load	p	$\overline{\sigma}_z$	$\overline{D}_z$	$\overline{B}_z$	$\overline{w}$	$\overline{\phi}$	$\overline{\psi}$
1	30	0.512219	0.003101	−0.030165	−14.8034	−0.92834	0.031699
	32	0.512227	0.003104	−0.030178	−14.8038	−0.92824	0.031700
2	30	0.005092	0.063811	−0.097001	−0.485768	7.56564	0.007404
	32	0.005092	0.063820	−0.096966	−0.485676	7.56496	0.007402
3	30	1.3645×10^{-4}	-8.1619×10^{-5}	0.762164	0.017022	0.006617	−0.045610
	32	1.3611×10^{-4}	-8.1620×10^{-5}	0.762115	0.017039	0.006617	−0.045607

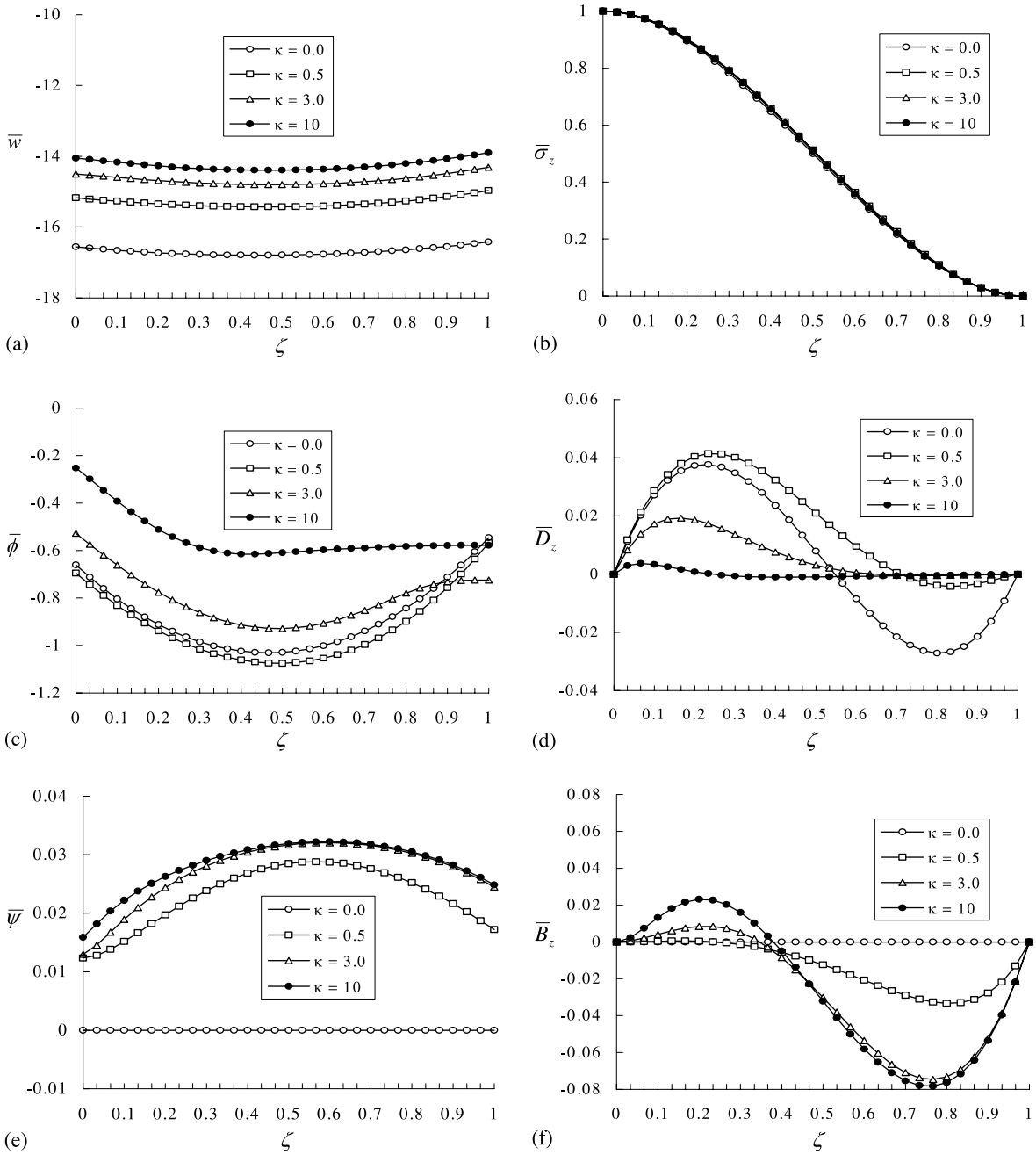

Fig. 2. Dimensionless quantities along the thickness direction for Load 1: (a) $\overline{w}$; (b) $\overline{\sigma}_z$; (c) $\overline{\phi}$; (d) $\overline{D}_z$; (e) $\overline{\psi}$; (f) $\overline{B}_z$.

Load 2, respectively. When the homogeneous $BaTiO_3$ plate is subjected to Load 3, however, the elastic and electric fields vanish as shown in Fig. 4a–d.

From the micromechanics study of Li (2000), it is known that for a two-phase $BaTiO_3$–$CoFe_2O_4$ composite, the magnetoelectric coefficients are not zero $(d_{11} \neq 0, d_{33} \neq 0)$ as a result of material synthesis,

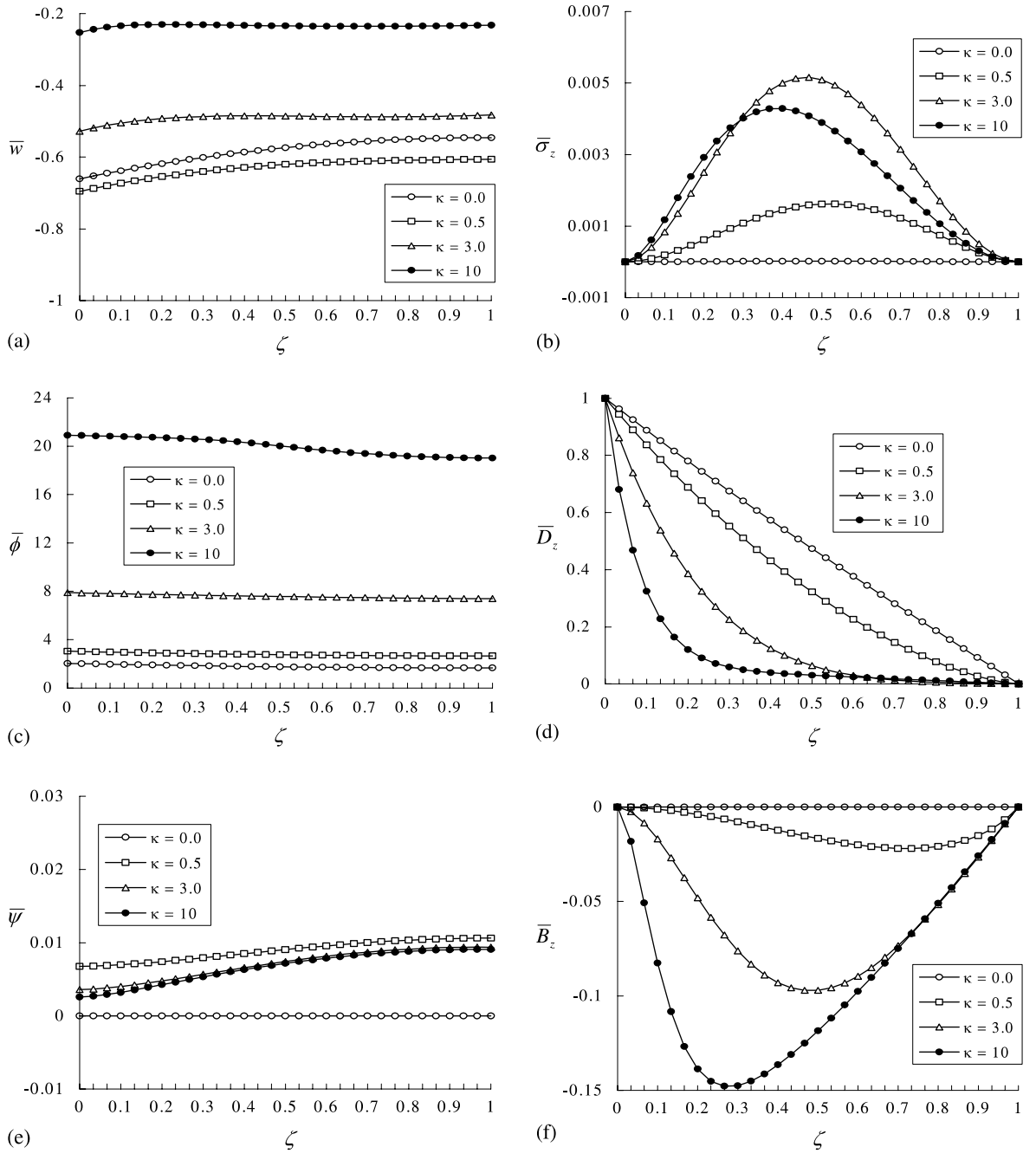

Fig. 3. Dimensionless quantities along the thickness direction for Load 2: (a) $\overline{w}$; (b) $\overline{\sigma}_z$; (c) $\overline{\phi}$; (d) $\overline{D}_z$; (e) $\overline{\psi}$; (f) $\overline{B}_z$.

although neither phase shows this coupling. The magnitude of the magnetoelectric coupling depends on the factors such as the material combination method and phase volume fraction. For a functionally graded material represented by Eq. (43), there is no simulation result of the magnetoelectric coupling available in

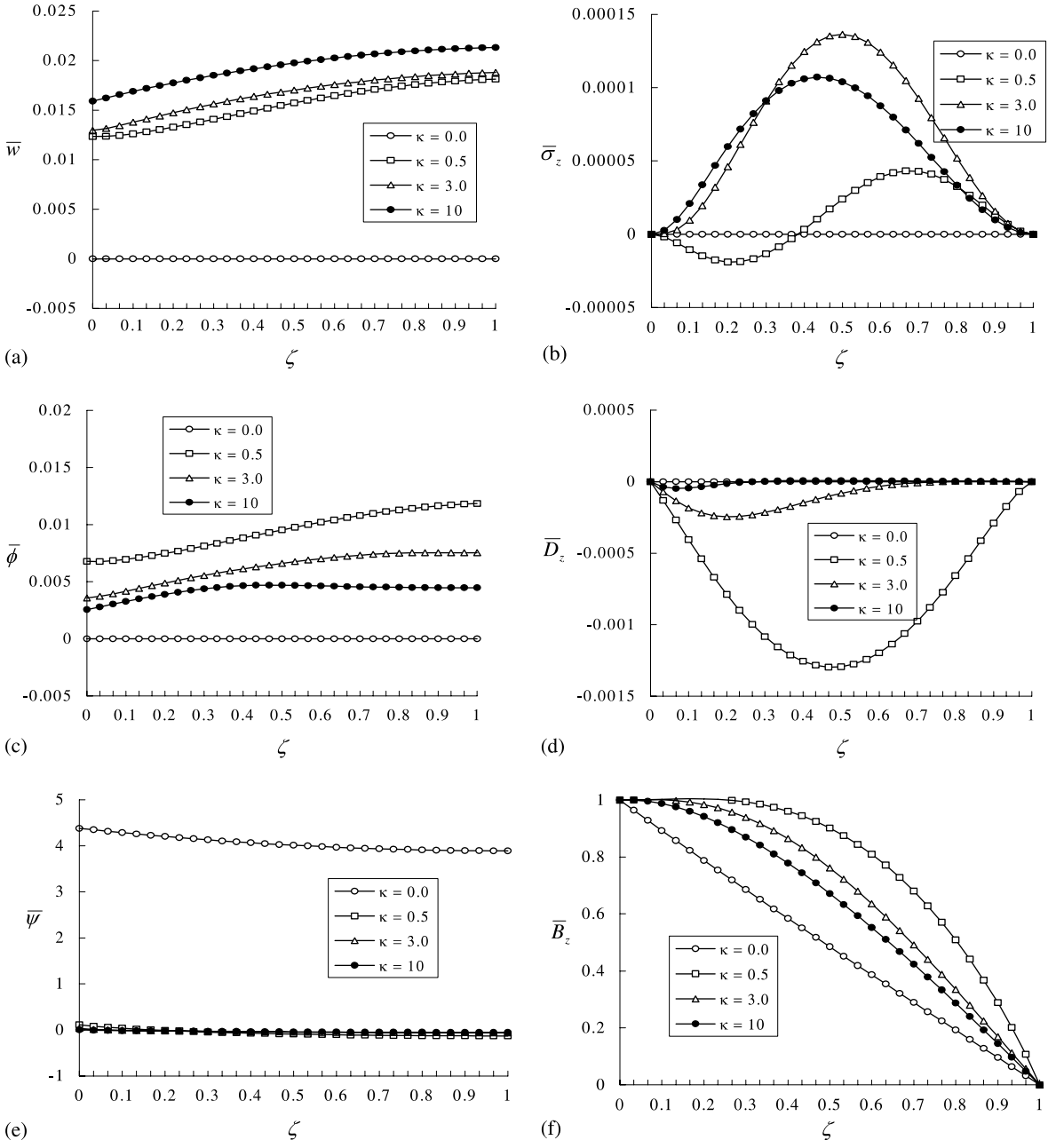

Fig. 4. Dimensionless quantities along the thickness direction for Load 3: (a) $\overline{w}$; (b) $\overline{\sigma}_z$; (c) $\overline{\phi}$; (d) $\overline{D}_z$; (e) $\overline{\psi}$; (f) $\overline{B}_z$.

literature. Li (2000) also pointed out that the theoretical prediction of the magnetoelectric coupling might be different from the experimental results. Nevertheless, our aim here is just to study the effect of this coupling on the behavior of the plate. Note that the material constants of the functionally graded plate represented by Eq. (43) vary from the ones of $BaTiO_3$ at the top surface to that of $CoFe_2O_4$ at the bottom

Table 2
Effect of magnetoelectric coupling on field variables ($\zeta = 0.8$)

Load	Coupling	$\overline{\sigma}_z$	$\overline{D}_z$	$\overline{B}_z$	$\overline{w}$	$\overline{\phi}$	$\overline{\psi}$
1	No	0.10866	−0.00044	−0.07329	−14.6226	−0.77997	0.03026
	Yes	0.10866	−0.00044	−0.07327	−14.6223	−0.77991	0.03027
2	No	0.00171	0.00592	−0.05155	−0.48740	7.43710	0.00912
	Yes	0.00171	0.00592	−0.05185	−0.48730	7.43690	0.00917
3	No	5.2019×10^{-5}	1.6617×10^{-6}	0.33459	0.01838	0.00750	−0.05681
	Yes	5.4436×10^{-5}	2.9223×10^{-6}	0.33459	0.01763	0.00892	−0.05681

surface continuously. Thus the two coefficients d_{11} and d_{33} are assumed to vary with the thickness direction in a way similar to that presented in Fig. 5(a) of Li (2000), which is approximately fitted as

$$d_{11}(\zeta) = 3.5\zeta_1^3 - 35\zeta_1^2 + 31.5\zeta_1$$
$$d_{33}(\zeta) = \begin{cases} -2250\zeta_1^2 + 5025\zeta_1, & \text{for } 0 \leqslant \zeta \leqslant 0.9 \\ -300000\zeta_1^2 + 543000\zeta_1 - 243000, & \text{for } 0.9 \leqslant \zeta \leqslant 1.0 \end{cases} \tag{44}$$

with the unit 10^{-12} N s/(VC), where $\zeta_1 = 1 - \zeta$. In addition, $\kappa = 3$ is selected for performing numerical calculation. Table 2 compares the nondimensional physical quantities at $\zeta = 0.8$ between the two cases, i.e. with and without the magnetoelectric coupling, respectively. As we can see, for the first two types of loads, the magnetoelectric coupling almost has no influence on the magneto-electro-elastic field in the plate. However, the situation changes for Load 3. In particular, there is an obvious effect on the electric field. For example, there is a relative error [1] about 15.9% of electric potential between the two cases, and it is up amount to 43.1% considering the electric displacement. To get a further knowledge, the distributions of $\overline{D}_z$ and $\overline{\phi}$ along the thickness direction are displayed in Figs. 5 and 6, respectively. We note that at about $\zeta = 0.2$, the electric displacement has its biggest negative value, for which the relative error between the two cases still has a value of 6.6%. While at $\zeta = 1$, the electric potential arrives its biggest value, for which the relative error is about 18.8%. It is obvious that when the plate is subjected to a magnetic load, the magnetoelectric coupling due to the mixture of the two phases should be taken into consideration.

6. Conclusions

By introducing two displacement functions and two stress functions, state equations with lower orders are derived in the paper. The thermal effect, body force, free charge density and electric current density are involved in the derivations. The separation of state equations will improve the computational efficiency for numerical calculations. In particular, the present method allows one to identify the physical essence of the problems. For example, when the plate is subjected to a normal mechanical force at the top or bottom surfaces, only the eighth-order state equation should be solved.

The state space formulations are also valid for a material with arbitrary nonhomogeneous properties along the axis of symmetry, for which an approximate laminate model is adopted to get a closed-form solution of the plate problem. It is also noted here that a similar model was ever employed by Fan and Zhang (1992), who dealt with a state equation with variable coefficients involving the

[1] Defined as: |(with − without)/with|.

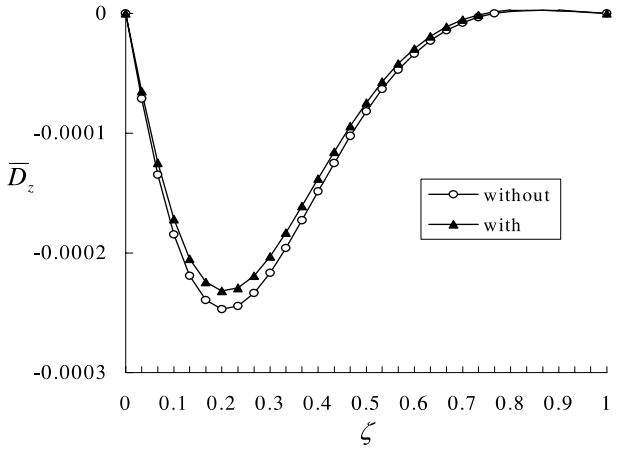

Fig. 5. Effect of magnetoelectric coupling on through thickness distribution of $\overline{D}_z$.

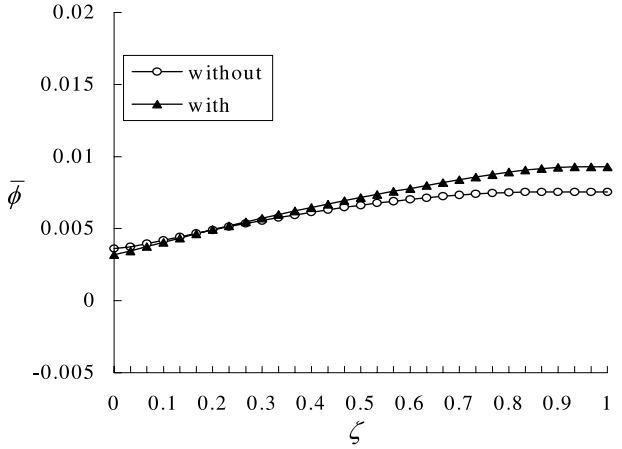

Fig. 6. Effect of magnetoelectric coupling on through thickness distribution of $\overline{\phi}$.

coordinate variable only. The analysis based on the approximate laminate model is very powerful since it can deal with arbitrary material inhomogeneity along the thickness direction. Furthermore, with the increase of layer number, the model will approach the actual structure and hence we can arrive at a solution of any expected precision. For a homogeneous or laminated plate with simply supported or rigidly slipping conditions, the solution presented in this paper is completely exact. Since no assumption on the magneto-electro-elastic field, such as those employed in plate theories, has been introduced except for the approximation due to the laminate model, the present analysis can serve as a three-dimensional benchmark to check various two-dimensional simplified theories and numerical methods.

The magnetoelectric coupling between the two phases $BaTiO_3$ and $CoFe_2O_4$ due to the material synthesis is discussed through the numerical investigation. We find that when the plate is subjected to a magnetic force, the influence of this coupling becomes significant on the electric field. This should be an important issue in practical design of magneto-electro-elastic structures with heterogeneous material properties.

Acknowledgements

The work was supported by the Natural Science Foundation of China (no. 10002016) and by the Korea Institute of Science and Technology Evaluation and Planning.

References

Avellaneda, M., Harshe, G., 1994. Magnetoelectric effect in piezoelectric/magnetostrictive multilayer (2–2) composites. Journal of Intelligent Material Systems and Structures 5, 501–513.

Bellman, R., 1970. Introduction to Matrix Analysis. McGraw-Hill, New York.

Chen, W.Q., Xu, R.Q., Ding, H.J., 1998. On free vibration of a piezoelectric composite rectangular plate. Journal of Sound and Vibration 218, 741–748.

Chen, W.Q., Ding, H.J., Xu, R.Q., 2001. Three-dimensional static analysis of multi-layered piezoelectric hollow spheres via the state space method. International Journal of Solids and Structures 38, 4921–4936.

Ding, H.J., Chen, W.Q., 2001. Three Dimensional Problems of Piezoelasticity. Nova Science Publishers, New York.

Ding, H.J., Chen, B., Liang, J., 1996. General solutions for coupled equations for piezoelectric media. International Journal of Solids and Structures 33, 2283–2298.

Ding, H.J., Chen, W.Q., Xu, R.Q., 2000. New state space formulations for transversely isotropic piezoelasticity with application. Mechanics Research Communications 27, 319–326.

Ezzat, M.A., Othman, M.I., 2000. Electromagneto-thermoelastic plane waves with two relaxation times in a medium of perfect conductivity. International Journal of Engineering Science 38, 107–120.

Fan, J.R., Ye, J.Q., 1990. An exact solution for the statics and dynamics of laminated thick plates with orthotropic layers. International Journal of Solids and Structures 26, 655–662.

Fan, J.R., Zhang, J.Y., 1992. Analytical solutions for thick, doubly curved, laminated shells. Journal of Engineering Mechanics 118, 1338–1356.

Huang, J.H., Chiu, Y.H., Liu, H.K., 1998. Magneto-electro-elastic Eshelby tensors for a piezoelectric-piezomagnetic composite reinforced by ellipsoidal inclusions. Journal of Applied Physics 83, 5364–5370.

Lee, J.S., Jiang, L.Z., 1996. Exact electroelastic analysis of piezoelectric laminae via state space approach. International Journal of Solids and Structures 33, 977–990.

Li, J.Y., 2000. Magneto-electro-elastic multi-inclusion and inhomogeneity problems and their applications in composite materials. International Journal of Engineering Science 38, 1993–2011.

Pagano, N.J., 1970. Exact solutions for rectangular bidirectional composites and sandwich plates. Journal of Composite Materials 4, 20–34.

Pan, E., 2001. Exact solution for simply supported and multilayered magneto-electro-elastic plates. Journal of Applied Mechanics 68, 608–618.

Reddy, J.N., Wang, C.M., Kitipornchai, S., 1999. Axisymmetric bending of functionally graded circular and annular plates. European Journal of Mechanics A/Solids 18, 185–199.

Tan, P., Tong, L.Y., 2002. Modeling for the electro-magneto-thermo-elastic properties of piezoelectric-magnetic fiber reinforced composites. Composites: Part A 33, 631–645.

Tanigawa, Y., 1995. Some basic thermoelastic problems for nonhomogeneous structural materials. Applied Mechanics Reviews 48, 287–300.

Tarn, J.Q., 2002. A state space formalism for anisotropic elasticity. Part I: Rectilinear anisotropy. International Journal of Solids and Structures 39, 5143–5155.

Wang, X., Shen, Y.P., 2002. The general solution of three-dimensional problems in magnetoelectroelastic media. International Journal of Engineering Science 40, 1069–1080.

Wang, X., Shen, Y.P., 2003. Inclusions of arbitrary shape in magnetoelectroelastic composite materials. International Journal of Engineering Science 41, 85–102.

Wang, J.G., Chen, L.F., Fang, S.S., 2003. State vector approach to analysis of multilayered magneto-electro-elastic plates. International Journal of Solids and Structures 40, 1669–1680.

Wu, C.C.M., Kahn, M., Moy, W., 1996. Piezoelectric ceramics with functional gradients: a new application in material design. Journal of American Ceramics Society 79, 809–812.